


 Cite this: *RSC Adv.*, 2020, **10**, 22234

# Purification, characterization, and hypoglycemic properties of eurocristatine from *Eurotium cristatum* spores in Fuzhuan brick tea†

 Gang Liu,<sup>abc</sup> Zhiguang Duan,<sup>abc</sup> Pan Wang,<sup>abc</sup> Daidi Fan <sup>abc</sup> and Chenhui Zhu <sup>\*abc</sup>

Fuzhuan brick tea (FBT) is a Chinese dark tea that is famous for its significant health benefits, in which *Eurotium cristatum* (*E. cristatum*) strains play a vital role in its postfermentation process. In this study, eurocristatine with hypoglycemic activity was discovered for the first time and purified from the spores of *E. cristatum* growing in FBT. Eurocristatine (98%) was obtained by D-101 macroporous resin-based column chromatography and preparative high performance liquid chromatography (HPLC) with a C<sub>18</sub> column as the stationary phase and 35% acetonitrile in ultrapure water as the mobile phase. Hypoglycemic activity in a Hep-G2 cell hypoglycemic model was used as a screening indicator during purification. The chemical structure of eurocristatine was characterized by ESI/MS, <sup>1</sup>H NMR and <sup>13</sup>C NMR analyses. The antidiabetic effects of eurocristatine were verified in high-fat diet/streptozocin-induced type 2 diabetes mellitus (T2DM) rats. The results showed that eurocristatine significantly reduced fasting blood glucose. Our study demonstrated that eurocristatine, as a newly discovered hypoglycemic active substance, could be considered a potential candidate for the treatment of diabetes and its complications.

 Received 17th April 2020  
 Accepted 2nd June 2020

DOI: 10.1039/d0ra03423a

[rsc.li/rsc-advances](http://rsc.li/rsc-advances)

## 1. Introduction

Fuzhuan brick tea (FBT) is widely studied and loved by people due to its unique pharmacological health benefits and pathological preventive effects, which has close ties with the growth of the dominant strain *E. cristatum* in the FBT postfermentation process. *E. cristatum*, a kind of probiotic, is nontoxic and safe, and the spores of FBT *E. cristatum* are capable of improving blood lipid metabolism, strengthening the immune system and have antioxidant and anticancer activity.<sup>1–4</sup> The spores can secrete multiple active metabolites during the process of golden flower blossoming.<sup>5–7</sup>

In recent years, biologically active metabolites have been isolated from *E. cristatum* spores of FBT, including flavonoids, proteases, alkaloids, diketopiperazines and polysaccharides.<sup>8–14</sup> These compounds show satisfactory biological activities, such as antibacterial activity, antiviral activity, antioxidant activity, and anticancer activity.<sup>15–17</sup> FBT extract can effectively prevent obesity in humans and experimental animals.<sup>18</sup> Studies have

shown that FBT has the ability to alleviate obesity and regulate intestinal flora in C57BL/6J mice fed a high-fat diet (HFD).<sup>19</sup> The effect of *E. cristatum*-containing black tea fermentation broth on the activities of digestive enzymes such as amylase, protease and lipase showed that black tea fermentation broth containing *E. cristatum* could significantly increase the activity of β-amylase and proteases and effectively reduce the activity of lipase.<sup>20</sup> However, most research has been limited to the extract or fermentation broth of FBT. It is not clear which specific substance plays a role in the above activities. *E. cristatum* was isolated from FBT and recultured separately to determine whether *E. cristatum* retained the above activities. Therefore, this research focused on the active metabolites of *E. cristatum* and their functions.

Previous studies in our laboratory found that blood glucose levels in diabetic mice were significantly lower than those in model mice after the feeding of spores of the FBT *E. cristatum* for 4 consecutive weeks by intragastric administration. Moreover, high doses of spores of the FBT *E. cristatum* showed no significant adverse reactions. It is necessary to investigate the active hypoglycemic substance in spore metabolites. In this research, we investigated methods to separate hypoglycemic active substances from the spores of FBT *E. cristatum* by macroporous resin and preparative high-performance liquid chromatography (HPLC), characterized the structure, verified the hypoglycemic activity of the active hypoglycemic substances, and solved the material basis of hypoglycemic activity from the spores of FBT *E. cristatum*. The quantitative analysis method using the identified hypoglycemic active substances as the

<sup>a</sup>Shaanxi Key Laboratory of Degradable Biomedical Materials, School of Chemical Engineering, Northwest University, Taibai North Road 229, Xi'an, Shaanxi, 710069, China. E-mail: zch2005@nwu.edu.cn; Fax: +86-29-88305118; Tel: +86-29-88305118

<sup>b</sup>Shaanxi R&D Center of Biomaterials and Fermentation Engineering, School of Chemical Engineering, Northwest University, Taibai North Road 229, Xi'an, Shaanxi, 710069, China

<sup>c</sup>Biotech & Biomed Research Institute, Northwest University, Taibai North Road 229, Xi'an, Shaanxi, 710069, China

† Electronic supplementary information (ESI) available. See DOI: 10.1039/d0ra03423a



indicator was established using analytical HPLC. This study will provide a scientific basis for the exploration and utilization of clinical hypoglycemic medicines.

## 2. Materials and methods

### 2.1. General experimental procedures

Fuzhuan brick tea was purchased from Xixian New District Qinyu Trading Co. Ltd, (Xi'an, China). The *E. cristatum* strain used was named XD-5 (obtained from the China General Microbiological Culture Collection Center). The process optimization steps for separating and purifying the hypoglycemic substance from the spores of *E. cristatum* are shown in Fig. 1. The main separation and purification methods were the use of D-101 macroporous resin-based column chromatography and preparative HPLC. D-101 macroporous resin was purchased from Beijing Green Herbs Science and Technology Development Co. Ltd (Beijing, China). The macroporous resin was food grade and was used directly for preparation. The acetonitrile used for HPLC analysis and ethanol used for preparative HPLC were of chromatography grade and purchased from Beijing Chemical Factory (Beijing, China). All other chemicals and reagents were of analytical grade and purchased from Beijing Chemical Factory. The preparative high-performance liquid chromatography equipment used was a Waters Prep 4000 liquid chromatography system. The analytical HPLC equipment used was a Shimadzu LC-20AT system. The electrospray ionization-mass spectrometry system (3200 Q-trap AB Sciex system consisting of a hybrid triple quadrupole/linear ion trap mass analyzer) and nuclear magnetic resonance (NMR) spectra (Swiss

Bruker AVANCE AV 400 superconducting pulse Fourier transform nuclear magnetic resonance spectrometer) were obtained from the Center of Analytical Test, Shenzhen Tsinghua University Research Institute.

### 2.2. Sample preparation and extraction

Ten grams of Fuzhuan brick tea was ground into a powder, and a suspension was prepared with physiological saline, inoculated onto PDA medium, and cultured for 5 to 7 days. Golden spores of *E. cristatum* were picked. The picked spores of *E. cristatum* were made into a spore suspension, the spore activity was  $1 \times 10^7$  cfu mL<sup>-1</sup>, 800  $\mu$ L of the suspension was inoculated onto a PDA plate, and golden yellow spores were obtained after 5 days. Fifty grams of spores were obtained in the previous step, and water was added to the extract at a ratio of 1 : 10 followed by sonication for 30 min. After centrifugation (5000 rpm, 30 min), the supernatant was collected, and this treatment was repeated three times according to this extraction method. The supernatant after three rounds of water leaching was combined to obtain the spore external extract.

### 2.3. Separation by D-101 resin-based column chromatography

D-101 macroporous resin needs to be pretreated before use. The resin was soaked in 500 mL of a 95% aqueous solution of ethanol overnight, and then the pretreated resin was placed on a sand core chromatography column (20  $\times$  300 mm). The fill height was 200 mm, and the column was eluted with 1 L of distilled water until the ethanol in the column was completely

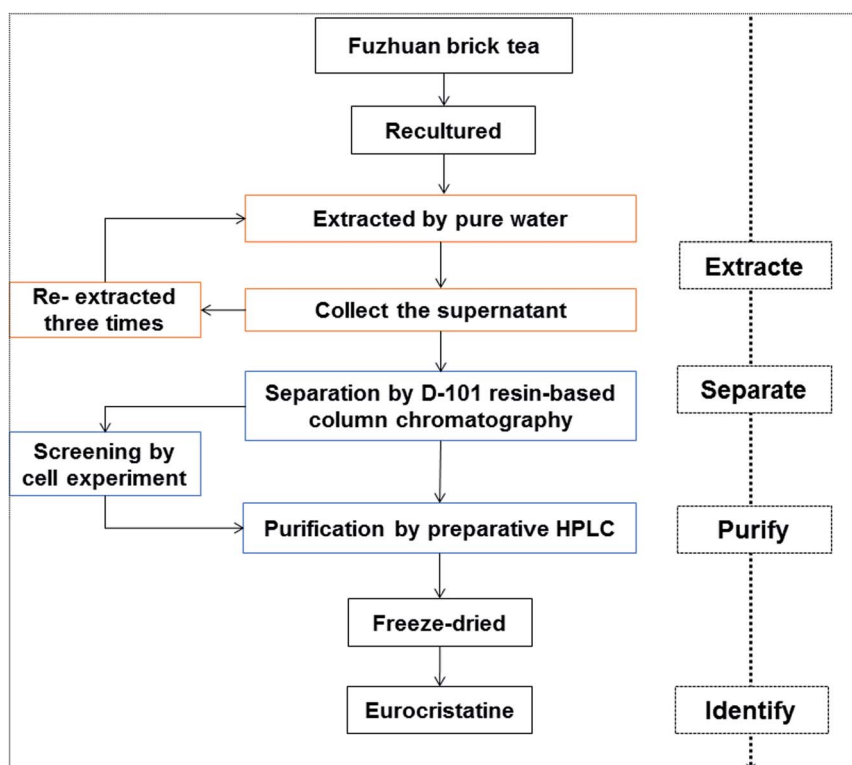


Fig. 1 Flow diagram of the purification process.



eluted. The spore external extract (200 mL, 50 mg mL<sup>-1</sup>) was loaded onto the pretreated chromatography column and adsorbed at a flow rate of 1 BV min<sup>-1</sup>. After adsorption was complete, 6 column volumes of deionized water at a flow rate of 2 BV min<sup>-1</sup> were used for equilibration, and then 0%, 10%, 20%, 30%, 40%, 50%, 60%, 70%, 80%, 90%, and 100% aqueous ethanol solutions were eluted at a flow rate of 1 BV min<sup>-1</sup> for 5 column volumes to obtain 11 different eluents. The obtained 11 eluents were concentrated and dried under vacuum at 50 °C using a rotary evaporator to obtain different extracts. The hypoglycemic activity of the 11 components was verified by the Hep-G2 cell model. The maximum dose concentration was set to 2 mg mL<sup>-1</sup> based on the crude aqueous extract concentration. The eluent of ethanol and water with the most significant hypoglycemic activity was selected for further separation and purification by preparative HPLC.

#### 2.4. Purification by preparative HPLC

In order to obtain a high purity product, a preparative HPLC purification method was performed. The flow rate was fixed at 30 mL min<sup>-1</sup>, the detection wavelength for monitoring was 235 nm, and 35% ethanol in ultrapure water was used as the mobile phase. The C<sub>18</sub> column (4.6 × 250 mm, 3.5 μm, Waters) served as the stationary phase for the preparative liquid phase. The sample solution was injected through a sample port onto the preparative HPLC column (20 mL). The maximum peak fraction was manually collected according to preparative HPLC chromatography and then concentrated and dried under vacuum at 40 °C using a rotary evaporator to obtain a monomer. Further verification of its hypoglycemic activity was carried out with the Hep-G2 cell model and animal experiments.

#### 2.5. Cell culture and treatments

Hep-G2 cells were cultured in medium supplemented with 10% bovine serum, 100 IU mL<sup>-1</sup> penicillin and 100 μg mL<sup>-1</sup> streptomycin at 37 °C in a 5% CO<sub>2</sub> atmosphere. When the cells grew to occupy 80% of the surface of the medium, the cells were washed with phosphate-buffered saline (PBS) twice, nitrified with trypsin and the number of cells were counted. Cells were seeded into a 96-well plate at a density of 1 × 10<sup>4</sup> cells per well with five wells left as blanks. Cells were incubated for 24 h, and the culture broth was decanted. Cells were incubated with normal glucose (5.5 mM) or high glucose (30 mM) plus insulin (100 nM) in the absence or presence of the extract at different concentrations for 24 h. Cells treated with normal glucose (5.5 mM) were used as blank controls, while cells treated with metformin (2 mM) were used as positive controls. The medium solution was removed 24 h later, and glucose consumption was calculated by the glucose concentrations of the blank wells minus the glucose concentrations in the plated wells. Cell viability was measured using the MTT method: MTT dilution (diluted with PBS to a final concentration of 5 mg mL<sup>-1</sup>) was added to each well at a ratio of MTT dilution : culture solution = 1 : 2. The cell pellet was dissolved in 150 μL of dimethyl sulfoxide for 10 min, and the absorbance was measured at 570 nm using a spectrophotometer.<sup>21</sup>

#### 2.6. Animal experiments

A total of 60 male 6 week-old specific pathogen-free SD rats (weighing 120 ± 20 g) were purchased from the Experimental Animal Center of the Fourth Military Medical University. Rats were given the first week to acclimate to their new environment and were given a normal diet. Following the acclimation period, rats were randomly divided into 2 groups: the Con group (rats fed basal diets, *n* = 10) and the HF group (rats fed high-sugar and high-fat diets, *n* = 50). After thirty days, the HF group rats received an intraperitoneal injection of fresh STZ solution (60 mg per kg body weight), and the fasting blood glucose levels were measured after 7 days. Rats with fasting blood glucose values ≥11.1 mmol L<sup>-1</sup> were considered diabetic rats and were randomly divided into 4 groups: the Mod group (rats fed high-sugar and high-fat diets, *n* = 10), Met group (rats fed high-sugar and high-fat diets and treated with 50 mg per kg body weight metformin, *n* = 10), ET-L group (rats fed high-sugar and high-fat diets and treated with 15 mg per kg body weight eucrostatine, *n* = 10), and ET-H group (rats fed high-sugar and high-fat diets and treated with 30 mg per kg body weight eucrostatine, *n* = 10). During the experiment, the fasting blood glucose levels of the rats were monitored and recorded weekly with a blood glucose meter (TD-3213A, Xiamen Raidmax Medical Devices Co., Ltd). The initial and final body weights of the rats were measured and recorded. The animals were euthanized and the livers were carefully removed. Liver sections were fixed with 10% neutral buffered formalin and embedded in paraffin.<sup>22</sup> Then, the samples was cut into 5 μm sections for hematoxylin and eosin (H&E) staining (Solarbio, Beijing, China). All images were captured under a TE 2000 fluorescence microscope (Nikon, Japan). All animal procedures were performed in accordance with the Guidelines for Care and Use of Laboratory Animals of Northwest University and approved by the Animal Ethics Committee of Northwest University (NWU-AWC-20190704M). All experiments met the requirements of the Laboratory Animal Act of the People's Republic of China.

#### 2.7. Identification of compound structure

Using DMSO-d<sub>6</sub> as the solvent, the prepared sample was diluted to a concentration of 500 μg mL<sup>-1</sup>. Identification of the purified compound was carried out by an electrospray ionization mass spectrometry (ESI/MS) system (3200 Q-trap AB Sciex system consisting of a hybrid triple quadrupole/linear ion trap mass analyzer) for quality and fragment pattern recognition. The spray voltage of the electrospray ion source was set to 4 kV, the ion source temperature was set to 300 °C, and nitrogen was used as the drying gas at a flow rate of 10 mL min<sup>-1</sup>.<sup>23,24</sup> Nuclear magnetic resonance (<sup>1</sup>H and <sup>13</sup>C NMR) spectra were obtained on a Swiss Bruker AVANCE AV 400 superconducting pulse Fourier transform nuclear magnetic resonance spectrometer. The chemical shifts of the protons and carbons were recorded on the δ scale of ppm. Hydrogen spectrum width: 6410.256 Hz (~16 ppm); carbon spectrum width 24 154.59 Hz (~240 ppm). All these identification results were obtained from analysts at the Analytical Testing Center of the Research Institute of Tsinghua University in Shenzhen, analysis method JY/T 007-



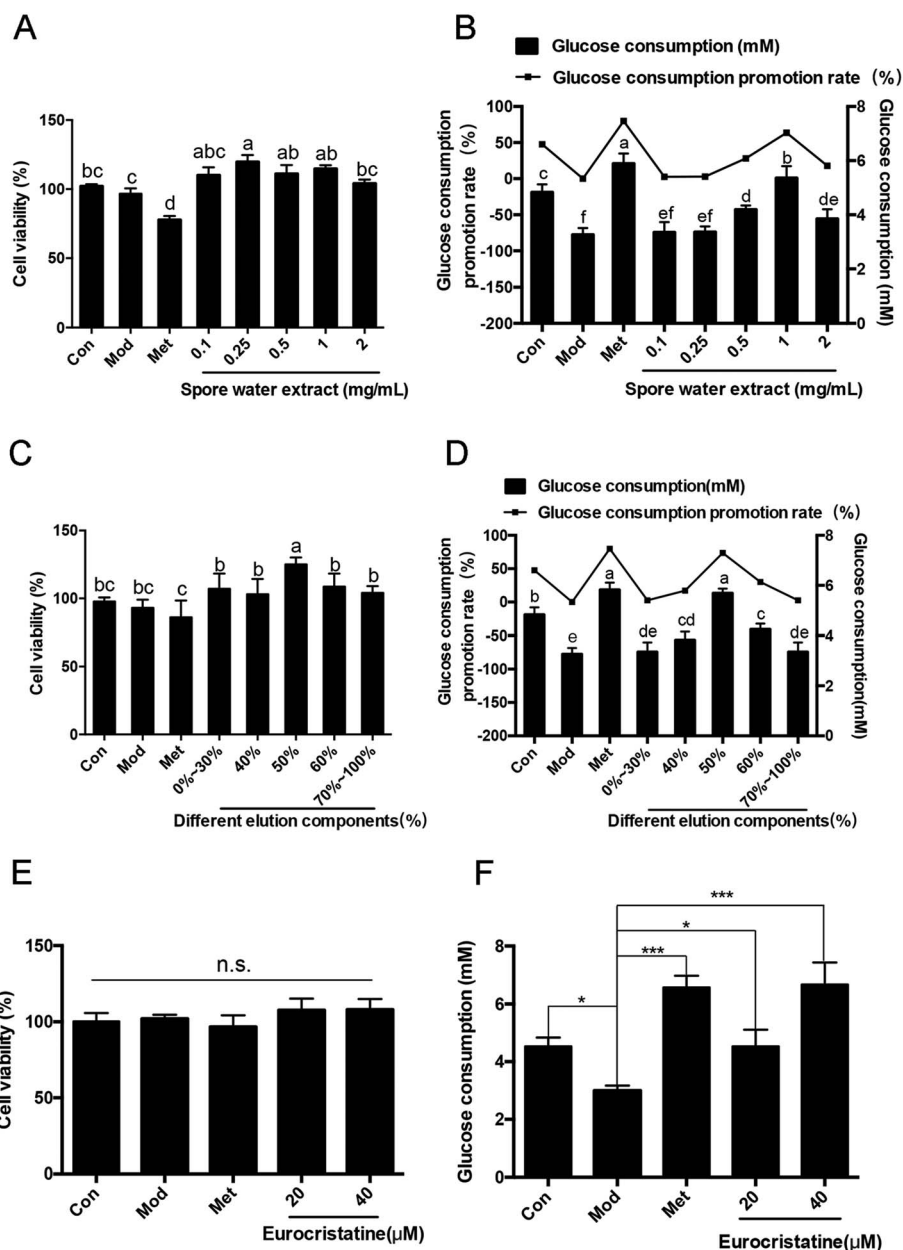


Fig. 2 Effects of the spore water extract (A and B), different elution components (C and D) and eurocrystatine (E and F) on glucose consumption and uptake in Hep-G2 cells with IR induced by high glucose and insulin. (A, C and E) Cell viability analyzed by MTT assays. (B, D and F) Glucose consumption and glucose consumption promotion rate from culture medium after 24 h of treatment in Hep-G2 cells. Vertical lines represent the standard deviations of five replicates. Values with different letters and a \* above are significantly different;  $P < 0.05$ , one-way ANOVA test.

1996, General principle of superconducting pulse Fourier transform nuclear magnetic resonance spectroscopy.

## 2.8. Analytical HPLC detection

Exploring a large number of experiments that analyzed liquid phase conditions, the HPLC analysis conditions of all the samples in this experiment were as follows: 35% acetonitrile in ultrapure water as the mobile phase, and a stationary phase of an analytical reversed-phase  $C_{18}$  column ( $4.6 \times 250$  mm,  $3.5 \mu\text{m}$ , Waters). The oven temperature was set to  $30^\circ\text{C}$ . The flow rate was  $1.0 \text{ mL min}^{-1}$ , the sample was filtered through a  $0.22 \mu\text{m}$  membrane filter, and a  $20 \mu\text{L}$  aliquot was injected onto the

column. The liquid phase of the sample was detected under UV at 235 nm. The eurocrystatine obtained in this experiment was dissolved in distilled water and formulated into 12.5, 25, 50, 100, and  $200 \mu\text{g mL}^{-1}$  solutions, and each standard solution was injected into the analytical HPLC in duplicate. A working calibration curve of the concentration and peak area of eurocrystatine was obtained for quantification of eurocrystatine in the spore extract.

## 2.9. Statistical analyses

All data are expressed as the mean  $\pm$  standard deviation (SD) of three independent experiments. One-way analysis of variance



(ANOVA) followed by Duncan's test was performed using SPSS version 19.0 software (SPSS Inc, IL, USA).  $n = 10$  per group rats were used in our study, statistical significance was considered at  $p < 0.05$ .

### 3. Results and discussion

#### 3.1. Hypoglycemic effects of the spore water extract

The above extracts were concentrated and dried under vacuum at 50 °C under vacuum to obtain 10 g of spore external extract. Then, the Hep-G2 cell hypoglycemic model was used to verify its hypoglycemic activity. The results of the hypoglycemic test of the spore water extract showed that the spore water extract from the spores of *E. cristatum* treatment exhibited an evident increase in glucose consumption, glucose uptake and glycogen content in model cells (Fig. 2B). Treatment with spore water extracts of 0.1, 0.25, 0.5, 1 and 2 mg mL<sup>-1</sup> alone for 24 h did not show any damage to Hep-G2 cell viability, which means that the spore water extracts had good biocompatibility (Fig. 2A). The desired hypoglycemic active substance is therefore present in the spore water extract. This is consistent with the previous theory that long-term drinking of brick boiled tea has the effect of hypoglycemia.<sup>25</sup>

#### 3.2. Resin-based column chromatography separation

We further separated the spore water extract through D-101 macroporous resin-based column chromatography. We used eleven different concentrations of ethanol and water eluent in this process: 0% ethanol in water eluent (not adsorbed) (3500 mg), 10% ethanol in water eluent (1865 mg), 20% ethanol in water eluent (1210 mg), 30% ethanol in water eluent (805 mg), 40% ethanol in water eluent (720 mg), 50% ethanol in water eluent (370 mg), 60% ethanol in water eluent (300 mg), 70% ethanol in water eluent (360 mg), 80% ethanol in water eluent (286 mg), 90% ethanol in water eluent (180 mg), and 100% ethanol eluent (270 mg). After separation by D-101 macroporous resin-based column chromatography, 370 mg (50% ethanol in water eluent) of the eurocrystatine-rich extract was obtained from 50 g of spores of FBT *E. cristatum*. The other eluents of ethanol in water did not show the absorption peak of eurocrystatine in the analyses of the spectra of the liquid phases. The analytical HPLC chromatograms of the spore external water extract and the eurocrystatine-rich extract are shown in Fig. 3A and B.

Then, the hypoglycemic activity of the 11 components was verified by the Hep-G2 cell model. Various components showed no cytotoxicity at doses of 0.05, 0.1, 0.25, 0.5, 1, and 2 mg mL<sup>-1</sup>, and cell viability was even higher than that of the normal group (Fig. 2C). Metformin was used as a positive control and showed a significant protective effect regarding the consumption of glucose. The effect was even higher than that of the control group, but the cell viability of metformin at the dose of 2 mM was significantly lower than that of the control group. Compared to the IR model, the 50% ethanol in water eluent significantly increased glucose consumption by 63.2% (Fig. 2D). Therefore, the preparative separation of hypoglycemic

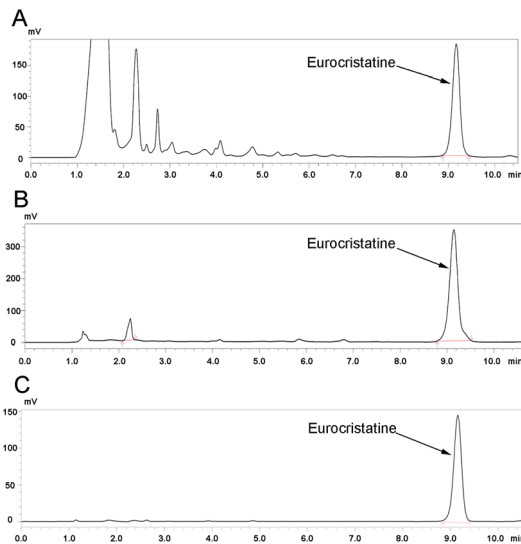


Fig. 3 The analytical HPLC chromatograms of the eurocrystatine product obtained by (A) crude extraction, (B) D-101 macroporous resin-based column chromatography and (C) preparative HPLC. The analytical HPLC column was a reversed-phase C18 column. The mobile phase was 35% acetonitrile in ultrapure water. The flow rate was 1.0 mL min<sup>-1</sup>. The column oven temperature was 30 °C. The detection wavelength was 235 nm.

substances from the spores of FBT *E. cristatum* could be primarily and cost-effectively achieved *via* adsorption and desorption on D-101 macroporous resin. Compared with other resin-based column chromatography separations,<sup>26,27</sup> the abovementioned method has the advantages of convenience, speed, and efficiency and can more quickly and efficiently isolate hypoglycemic substances from spore water extracts.

#### 3.3. Preparative HPLC purification

Purification was performed on a preparative HPLC system, and the flow rate, mobile phase and sample loading amount are important parameters for enhancing selectivity and capacity.<sup>28</sup> When fixing the flow rate at 30 mL min<sup>-1</sup>, the most efficient purification of the eurocrystatine-rich extract was obtained by using 35% ethanol in ultrapure water as the mobile phase at a sample loading amount of 50 mg. On the basis of the above conditions, 370 mg of the eurocrystatine-rich extract (approximately 7 injections) was purified by preparative HPLC, yielding 250 mg of 98% pure eurocrystatine product. An *in vitro* hypoglycemic assay of eurocrystatine was performed as described above. The results show that the dose of MET and eurocrystatine had low cytotoxicity compared to the control (Fig. 2E), which demonstrated that a model of IR in Hep-G2 cells was successfully built. Moreover, eurocrystatine significantly increased glucose consumption by 77.5% and 126.7% at 20 and 40 μM, respectively (Fig. 2F). A standard curve was developed using the purified eurocrystatine to allow for quantification of eurocrystatine in the extracts of the spores of *E. cristatum* by analytical HPLC, which showed that eurocrystatine content and its peak area show an excellent linear relationship (Fig. S1†). The analytical HPLC chromatograms of the eurocrystatine product obtained by



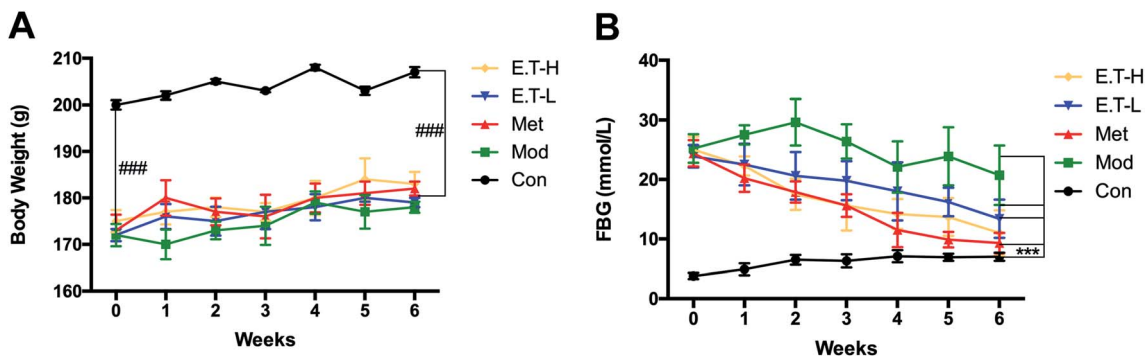


Fig. 4 Effect of eurocristatine on body weight (A) and the blood glucose level (B) in type 2 diabetic rats treated with 15 and 30 mg kg<sup>-1</sup> eurocristatine. Each value is expressed as the mean  $\pm$  SD ( $n = 10$  per group). The results were statistically analyzed with one-way ANOVA. \* and # indicate significantly different values ( $P < 0.05$ ). \* $P < 0.05$ , \*\* $P < 0.01$ , \*\*\* $P < 0.001$ , # $P < 0.05$ , ## $P < 0.01$ , ### $P < 0.001$ .

preparative HPLC are shown in Fig. 3C. Analytical HPLC analysis of the purified compound showed a single peak, accounting for 98% of the total detectable peak area. The analytical HPLC chromatograms of the spore external water extract and the eurocristatine-rich extract showed the single peak at the same position. As observed from the above results, eurocristatine from the spores of FBT *E. cristatum* exhibited stronger anti-hyperglycemic activity. Remarkably, the high antihyperglycemic activities of the water extracts corresponding to their high glucose consumption promotion rate values coincided with the high purity of eurocristatine in the extracts. This shows that eurocristatine plays an important role in the hypoglycemic process of the spores of the FBT *E. cristatum*.

### 3.4. Hypoglycemic activity in diabetic rats

To investigate the effects of eurocristatine on the development of diabetes, we measured the body weight and levels of blood glucose in high-fat diet fed STZ-induced diabetic rats. As shown in Fig. 4A, the body weights of all STZ-injected groups were lower than those of the normal control group. The body weights of the rats in the Met group, ET-L group and ET-H group were basically the same as that of the Mod group, which indicates that eurocristatine itself does not cause significant weight loss in rats. The effect of eurocristatine administration on blood glucose levels in diabetic rats is shown in Fig. 4B. Eurocristatine administration resulted in a significant reduction in FBG in diabetic rats. After 6 weeks of treatment, the blood glucose levels in the ET-L and ET-H

groups significantly decreased to 43.9 and 56.0%, respectively, when compared to the Mod group. These data showed that eurocristatine treatments can help to alleviate the diabetic symptoms of FBG reduction. This result further proves that eurocristatine, as a natural product,<sup>29–31</sup> has the advantages of being nontoxic and efficient in lowering blood sugar.

As shown in Fig. 5, the histological examination exhibited that the structure of the liver lobule were visible in the Con group, the liver cell border were clear, and the nucleus were located in the center of cells, besides, the hepatic cord around the central vein were arranged neatly. In the Mod group, the liver lobular structure disappeared with a large amount of lipid accumulation, and the structure of the hepatic cord were disordered, and the liver tissue had the obvious pathological lesions. Researches had shown that hyperglycemia and hepatic steatosis were occurred in most cases of T2DM,<sup>32</sup> which was consistent with the results we observed in our study. However, after treatment by metformin, ET-L, and ET-H, these abnormalities were all reversed. These above results indicated that hepatic steatosis and hyperglycemia were simultaneously improved by anti-diabetic agents administration in diabetic rats,<sup>33</sup> which indicated that eurocristatine had the significant hepatoprotective effect of diabetic rat, and might be conducive to improve the abnormal glucose metabolism.

### 3.5. Confirmation of purified the eurocristatine product

The chemical structure of the purified product was verified by ESI/MS, <sup>1</sup>H NMR and <sup>13</sup>C NMR analyses. The ESI/MS spectrum (Fig. 6A and B), <sup>1</sup>H NMR spectrum (Fig. 6C) and <sup>13</sup>C NMR spectrum (Fig. 6D) were as follows. The ESI/MS spectrum (Fig. 6A) (negative ion) of the sample showed an  $m/z$  of 567.2249, consistent with the ESI/MS spectrum of the test sample ( $[M - H]^-$   $m/z$  567.2720). The ESI/MS spectrum (Fig. 6B) (positive ion) of the sample showed an  $m/z$  of 591.2757, which is consistent with the sample  $[M + Na]^+$   $m/z$  of 591.2696. The <sup>1</sup>H NMR spectrum shows a total of 18 proton signals, which is the same as the number of protons in the sample tested;  $\delta$ : 8.25 (1H, s), 7.38 (1H, d, 7.2 Hz), 7.01 (1H, dd, 8.0, 8.0 Hz), 6.71 (1H, s), 6.62 (1H, dd, 8.0, 8.0 Hz), 6.59 (1H, d, 8.0 Hz), 4.89 (1H, br s), 4.11 (1H, t), 3.38 (1H, br s), 3.12 (1H, br s), 2.38 (1H, dd, 14.0, 9.5 Hz), 1.93 (1H, m), 0.79 (3H, d, 6.4 Hz), and 0.68 (3H, d, 6.0 Hz), combined

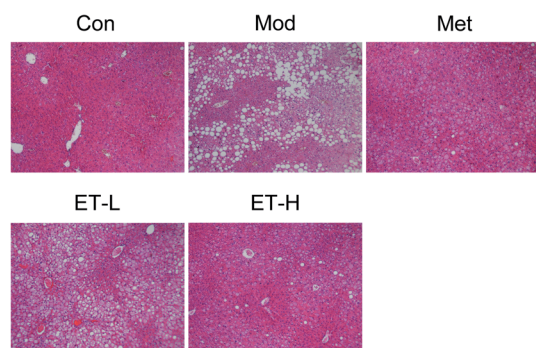


Fig. 5 Effects of eurocristatine on histological examination (100 $\times$ ).



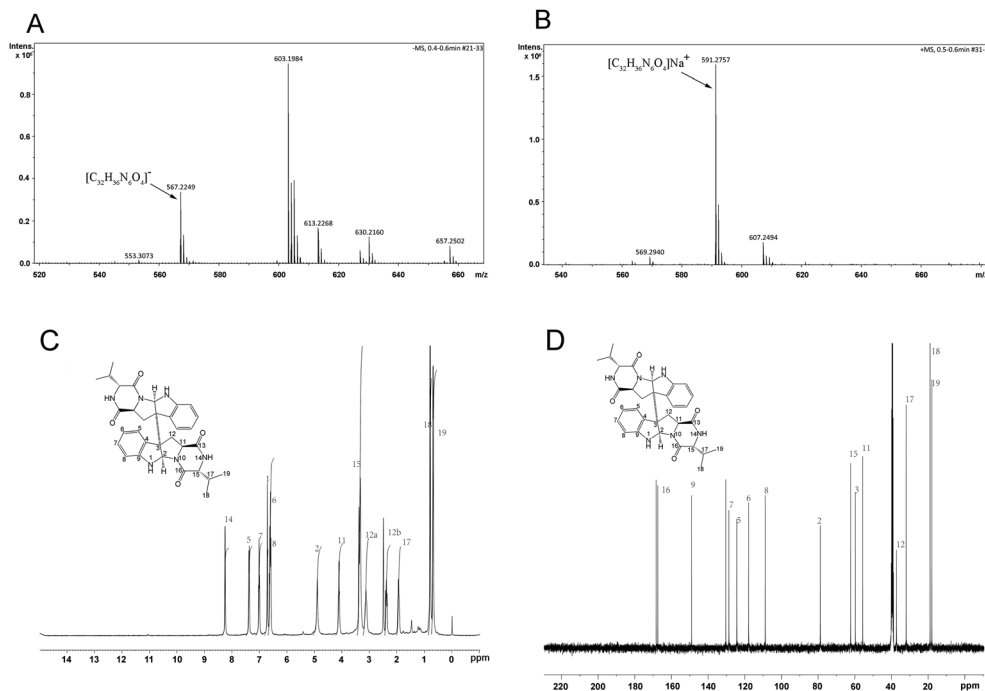


Fig. 6 The ESI/MS spectrum of the eurocristatine product negative ion mode:  $M - H$ :  $m/z$  567.2720 (A) and positive ion mode:  $M + Na$ :  $m/z$  591.2696 (B) purified by preparative HPLC. NMR spectra (DMSO, 600 MHz) of the eurocristatine product purified by preparative HPLC:  $^1H$  NMR spectrum (C) and  $^{13}C$  NMR spectrum (D).

with the HSQC spectrum (Fig. S2<sup>†</sup>), where  $\delta$ : 8.25 (1H, s) and 6.71 (1H, s) are the lively NH proton signals. The  $^{13}C$  NMR spectrum showed a total of 16 effective monomer peaks, and combined with the hydrogen and DEPT spectra (Fig. S3<sup>†</sup>), there were 5 quaternary carbons, combined with two-dimensional spectrum-assisted carbon spectrum analysis as follows: 16 effective monomer peaks, of which 8 are tertiary carbon peaks, 1 secondary carbon peak, 5 quaternary carbon peaks, and 2 primary carbons. The  $^1H$  NMR spectral data and the  $^{13}C$  NMR spectral data are shown in the ESI<sup>†</sup> (Table S1 and S2<sup>†</sup>). In summary, after spectroscopy by ESI/MS,  $^1H$  NMR,  $^{13}C$  NMR and 2D NMR, the NMR data of the sample structure for measurement are quite consistent with the NMR data of the eurocristatine structure reported in the literature,<sup>13</sup> and the structure of the sample to be tested was determined to be eurocristatine (Fig. 7), which is a diketopiperazine dimer.

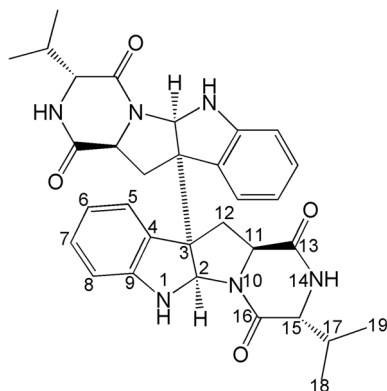


Fig. 7 Structure of eurocristatine.

Previous studies showed that several diketopiperazine dimers have been reported from fungal sources.<sup>34–36</sup> However, eurocristatine as a diketopiperazine dimer was isolated for the first time from *E. cristatum* spores of FBT.

## 4. Conclusion

In conclusion, this is the first report of the hypoglycemic active substance isolated from the spores of FBT *E. cristatum* to be identified as eurocristatine, which can be used as a medicine for the prevention and treatment of diabetes and its complications. In this paper, a D-101 macroporous resin-based column chromatography method was developed to yield highly pure eurocristatine from the spores of FBT *E. cristatum*, which demonstrated satisfactory hypoglycemic activity. The methods mentioned above in this study would be easy to scale-up for industrial application. However, as this is the first study to identify the hypoglycemic properties of eurocristatine, and the mechanism of the hypoglycemic action of eurocristatine remains to be further explored.

## Conflicts of interest

The authors declare no conflict of interest.

## Acknowledgements

This research was funded by the National Natural Science Foundation of China (21878247, 21776227, 21808184); Shaanxi Key Laboratory of Degradable Biomedical Materials Program (2014SZS07-Z01).



## References

- 1 W. W. May Zin, S. Buttachon, T. Dethoup, J. A. Pereira, L. Gales, Á. Inácio, P. M. Costa, M. Lee, N. Sekeroglu, A. M. S. Silva, M. M. M. Pinto and A. Kijjoa, *Phytochemistry*, 2017, **141**, 86–97.
- 2 A. P. Almeida, T. Dethoup, N. Singburauodom, R. Lima, M. H. Vasconcelos, M. Pinto and A. Kijjoa, *J. Nat. Pharm.*, 2010, **1**, 25–29.
- 3 Y. Ishikawa, K. Morimoto and T. Hamasaki, *J. Am. Oil Chem. Soc.*, 1984, **61**, 1864–1868.
- 4 J. Gao, M. M. Radwan, F. León, X. Wang, M. R. Jacob, B. L. Tekwani, S. I. Khan, S. Lupien, R. A. Hill and F. M. Dugan, *Med. Chem. Res.*, 2012, **21**, 3080–3086.
- 5 H.-H. Li, L.-Y. Luo, J. Wang, D.-H. Fu and L. Zeng, *Food Res. Int.*, 2019, **120**, 275–284.
- 6 Y. Rui, P. Wan, G. Chen, M. Xie, Y. Sun, X. Zeng and Z. Liu, *Lebensm.-Wiss. Technol.*, 2019, **110**, 168–174.
- 7 A. Xu, Y. Wang, J. Wen, P. Liu, Z. Liu and Z. Li, *Int. J. Food Microbiol.*, 2011, **146**, 14–22.
- 8 X. Xu, H. Mo, M. Yan and Y. Zhu, *J. Sci. Food Agric.*, 2007, **87**, 1502–1504.
- 9 Y. Xiao, K. Zhong, J.-R. Bai, Y.-P. Wu, J.-Q. Zhang and H. Gao, *Lebensm.-Wiss. Technol.*, 2020, **117**, 108629.
- 10 G. J. Slack, E. Puniani, J. C. Frisvad, R. A. Samson and J. D. Miller, *Mycol. Res.*, 2009, **113**, 480–490.
- 11 M. Podojil, P. Sedmera, J. Vokoun, V. Betina, H. Baráthová, Z. Ďuračková, K. Horáková and P. Nemeč, *Folia Microbiol.*, 1978, **23**, 438–443.
- 12 O. Smetanina, A. Kalinovskii, Y. V. Khudyakova, N. Slinkina, M. Pivkin and T. Kuznetsova, *Chem. Nat. Compd.*, 2007, **43**, 395–398.
- 13 N. M. Gomes, T. Dethoup, N. Singburauodom, L. Gales, A. M. S. Silva and A. Kijjoa, *Phytochem. Lett.*, 2012, **5**, 717–720.
- 14 X. Zou, Y. Li, X. Zhang, Q. Li, X. Liu, Y. Huang, T. Tang, S. Zheng, W. Wang and J. Tang, *Molecules*, 2014, **19**, 17839–17847.
- 15 F. Y. Du, X. M. Li, C. S. Li, S. Zhuo and B. G. Wang, *Bioorg. Med. Chem. Lett.*, 2015, **43**, 4650–4653.
- 16 F. Y. Du, L. Xin, L. Xiao-Ming, Z. Li-Wei and W. Bin-Gui, *Mar. Drugs*, 2017, **15**, 24.
- 17 Y. Li, K. L. Sun, Y. Wang, P. Fu, P. P. Liu, C. Wang and W. M. Zhu, *Chin. Chem. Lett.*, 2013, **24**, 1049–1052.
- 18 D. Kang, M. Su, Y. Duan and Y. Huang, *Food Funct.*, 2019, **10**(8), 5032–5045.
- 19 G. Chen, M. Xie, Z. Dai, P. Wan and Y. Sun, *Mol. Nutr. Food Res.*, 2018, **62**, 1700485.
- 20 Q. Huang, *Microbiology*, 2007, **34**, 917–920.
- 21 F. Yan, G. Dai and X. Zheng, *J. Nutr. Biochem.*, 2016, **36**, 68–80.
- 22 H. Yin, L. Huang, T. Ouyang and L. Chen, *Int. Immunopharmacol.*, 2018, **55**, 55–62.
- 23 K. Sichilongo, Z. G. Keolopile, S. Ndlovu, E. Mwando, C. Shaba and A. Masele, *Int. J. Mass Spectrom.*, 2016, **410**, 1–11.
- 24 R. Cherfia, A. Zaiter, S. Akkal, P. Chaimbault, A. B. Abdelwahab, G. Kirsch and N. Kacem Chaouche, *Bioorg. Chem.*, 2020, **96**, 103535.
- 25 Q. Li, Z. Liu, J. Huang, G. Luo and J. Hu, *J. Sci. Food Agric.*, 2013, **93**, 1310–1316.
- 26 L. Sun, Y. Guo, C. Fu, J. Li and Z. Li, *Food Chem.*, 2013, **136**, 1022–1029.
- 27 G. Wang, W. Chen, J. Hu, B. Fan, J. Shi and J. Xu, *J. Chromatogr. B: Anal. Technol. Biomed. Life Sci.*, 2019, **1110–1111**, 43–50.
- 28 P. Kuang, D. Song, Q. Yuan, R. Yi, X. Lv and H. Liang, *Food Chem.*, 2013, **136**, 342–347.
- 29 S. Deshaware, S. Gupta, R. S. Singhal, M. Joshi and P. S. Variyar, *Food Chem.*, 2018, **262**, 78–85.
- 30 B. Arumugam, T. Manaharan, C. K. Heng, U. R. Kuppasamy and U. D. Palanisamy, *LWT–Food Sci. Technol.*, 2014, **59**, 707–712.
- 31 S. R. Naik, J. M. B. Filho, J. N. Dhuley and V. Deshmukh, *J. Ethnopharmacol.*, 1991, **33**, 37–44.
- 32 Z. Sun and M. A. Lazar, *Trends Endocrinol. Metab.*, 2013, **24**, 4–12.
- 33 M.-S. Kim, S.-H. Kim, S.-J. Park, M. J. Sung, J. Park, J.-T. Hwang, H. J. Yang, S. Kim, D. Seo, S. S. Shin and H. J. Hur, *J. Funct. Foods*, 2017, **35**, 295–302.
- 34 S. Cai, X. Kong, W. Wang, H. Zhou, T. Zhu, D. Li and Q. Gu, *Cheminform*, 2012, **53**, 2615–2617.
- 35 R. Raju, A. M. Piggott, M. Conte, W. G. L. Aalbersberg and R. J. Capon, *Org. Lett.*, 2009, **11**, 3862–3865.
- 36 G. Y. Li, T. Yang, Y.-G. Luo, X.-Z. Chen, D.-M. Fang and G.-L. Zhang, *Org. Lett.*, 2009, **11**, 3714–3717.

